Ultrastrong Absorption Meets Ultraweak Absorption: Unraveling the Energy-Dissipative Routes for Dye-Sensitized Upconversion Luminescence

Xue, B.; Wang, D.; Tu, L.; Sun, D.; Jing, P.; Chang, Y.; Zhang, Y.; Liu, X.; Zuo, J.; Song, J.; Qu, J.; Meijer, E.J.; Zhang, H.; Kong, X.

DOI
10.1021/acs.jpclett.8b01931

Publication date
2018

Document Version
Final published version

Published in
Journal of Physical Chemistry Letters

THE JOURNAL OF PHYSICAL CHEMISTRY Letters

Cite This: J. Phys. Chem. Lett. 2018, 9, 4625−4631

Letter

pubs.acs.org/JPCL

Ultrastrong Absorption Meets Ultraweak Absorption: Unraveling the Energy-Dissipative Routes for Dye-Sensitized Upconversion Luminescence

Bin Xue,[†,‡] Dan Wang,[†] Langping Tu,[‡,∥] Dapeng Sun,[∥] Pengtao Jing,[‡] Yulei Chang,[‡] Youlin Zhang,*[,‡] Xiaomin Liu,[‡] Jing Zuo,[‡,§,∥] Jun Song,*[,†] Junle Qu,*[,†] Evert Jan Meijer,[∥] Hong Zhang,[∥] and Xianggui Kong*[,‡]

[†]Key Lab of Optoelectronics Devices and Systems of Ministry of Education/Guangdong Province, Shenzhen University, 518060 Shenzhen, China

[‡]State Key Laboratory of Luminescence and Applications, Changchun Institute of Optics, Fine Mechanics and Physics, Chinese Academy of Sciences, Changchun 130033, China

[§]Graduate University of the Chinese Academy of Sciences, Beijing 100049, China

[∥]Van't Hoff Institute for Molecular Sciences, University of Amsterdam, Science Park 904, 1098 XH Amsterdam, The Netherlands

Supporting Information

ABSTRACT: Dye sensitization is becoming a new dimension to highly improve the upconversion luminescence (UCL) of lanthanide-doped upconversion nanoparticles (UCNPs). However, there is still a lack of general understanding of the dye−UCNPs interactions, especially the confused large mismatch between the inputs and outputs. By taking dye-sensitized $NaYF_4$:Yb/Er@$NaYF_4$:Nd UCNPs as a model system, we not only revealed the in-depth energy-dissipative process for dye-sensitized UCL but also confirmed the first ever experimental observation of the energy back transfer (EBT) in the dye-sensitized UCL. Furthermore, this energy-dissipative EBT restricted the optimal ratio of dyes to UCNP. By unearthing all of the energy loss behind the EBT, energy transfer, and energy migration processes, this paper sheds light on the further design of effective dye-sensitized nanosystems for UCL or even downconversion luminescence.

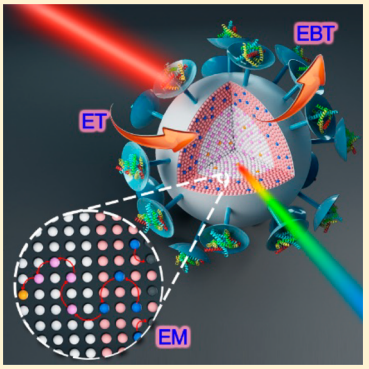

Energy transfer (ET) of photons is generally reserved for flows of excitation energy from a donor to a proximate or remote acceptor, transferring the energy to a suitable position or utilizable energy region, which is vital for solar cells, photosynthesis, and biophotonic applications.[1−3] Recently, such applications have fully aroused a renaissance due to the fact that the fundamental process of ET could be exquisitely manipulated on the nanoscale. A typical example is lanthanide ion (Ln^{3+})-doped upconversion nanoparticles (UCNPs), which effectively convert near-infrared (NIR) light into the visible region through adjustment of the ratios, concentrations, species, and positions in the nanoregion. Their use has been propelled in various fields including bioimaging,[4,5] sensing,[6−8] optical encoding,[9,10] super-resolution nanoscopy,[11,12] optogenetics,[13,14] and nanomedicine-based applications.[15−18] However, the weak upconversion luminescence (UCL) of UCNPs severely hampers their further practical usage. This weak UCL mainly arises from the ultraweak absorption coefficients ($\varepsilon \approx 0.1$ to 10 M^{-1} cm^{-1}) of lanthanide ions (Ln^{3+}), which results in the overall excited-state population of UCNPs remaining at an ultralow level. Therefore, acquiring a highly excited-state population for UCNPs is always an intractable issue.

Innovative ways, such as coating the nanoshell,[19,20] using laser cavity,[21] surface-plasmon coupling,[22−24] and even high-power excitation,[25] significantly increase the excited-state population of UCNPs to increase the UCL intensity. In particular, recently, Hummelen et al. utilized dye antennas to increase the excited-state population of UCNPs through the Förster resonance energy transfer (FRET) mechanism.[26] Very recently, this strategy has been further developed by incorporating other kinds of dyes or Ln^{3+} ions to maximize the spectra overlap,[27−29] which introduced more ET to enhance UCL. Very recently, dye-sensitized downconversion luminescence (DCL) has also been fulfilled.[30] Accordingly, dye sensitization of Ln^{3+}-doped nanoparticles opens great opportunities for many applications.[31−33]

At present, existing studies demonstrated either increased UCL or increased excitation range, and there is still a lack of general understanding of the dye−UCNPs interactions, with many remaining problems to be solved. For example, we know that the ultrastrong absorption of one NIR dye is comparable

Received: June 20, 2018
Accepted: August 1, 2018
Published: August 1, 2018

DOI: 10.1021/acs.jpclett.8b01931
J. Phys. Chem. Lett. 2018, 9, 4625−4631

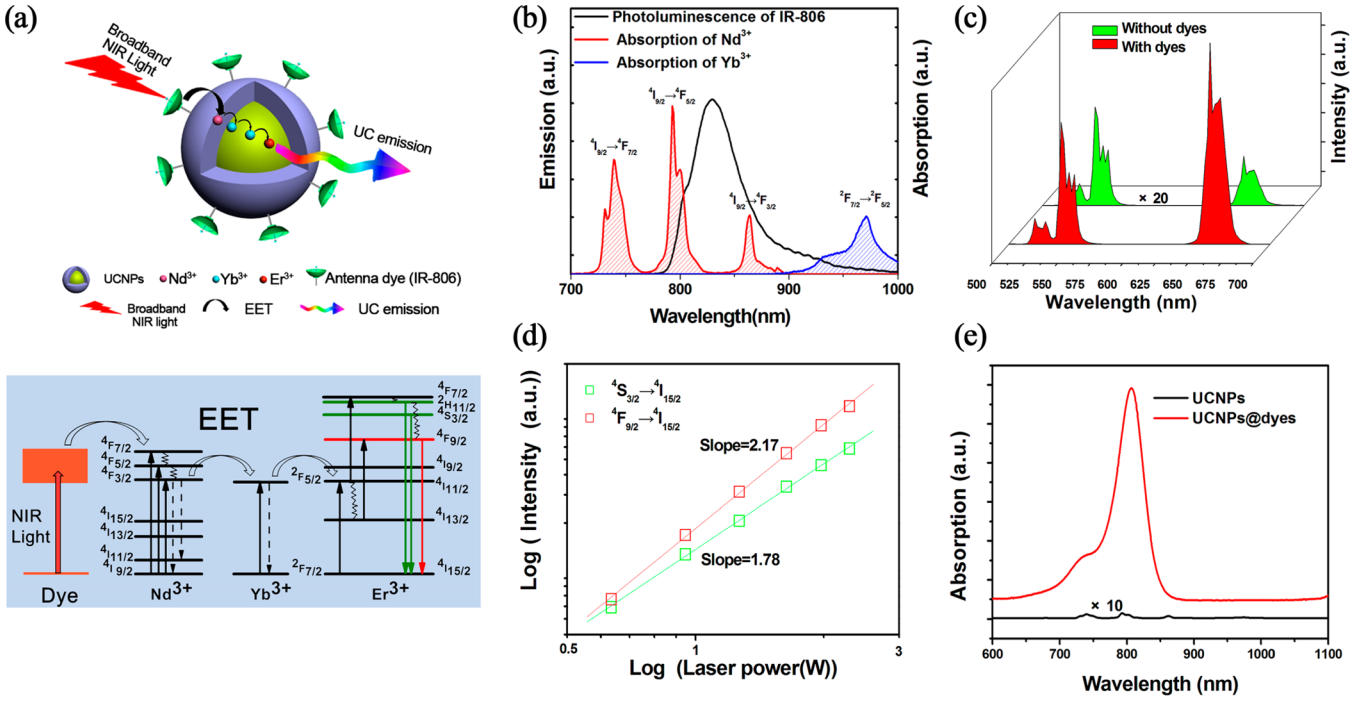

Figure 1. (a) Schematic diagram illustrating the UCL of IR-806 sensitized core−shell UCNPs based on an excitation energy transportation mechanism and simplified energy-level diagrams illustrating the energy-transfer process. Key: EET: excitation energy transportation; NIR: near-infrared; and UC: upconversion. (b) Emission spectrum of IR-806 under excitation of 808 nm in $CHCl_3$ (black line), absorption spectra of Nd^{3+} (red line), and Yb^{3+} (blue line). (c) UCL of Nd20 CS and the dye-sensitized Nd20 CS under an excitation of 808 nm (8.3 W/cm^2). (d) Log−log plots of the UCL intensity versus laser power for the green and red emissions of the dye-sensitized Nd20 CS under excitation of 808 nm. (e) Absorption spectra of Nd20 CS (black line) and dye-sensitized Nd20 CS.

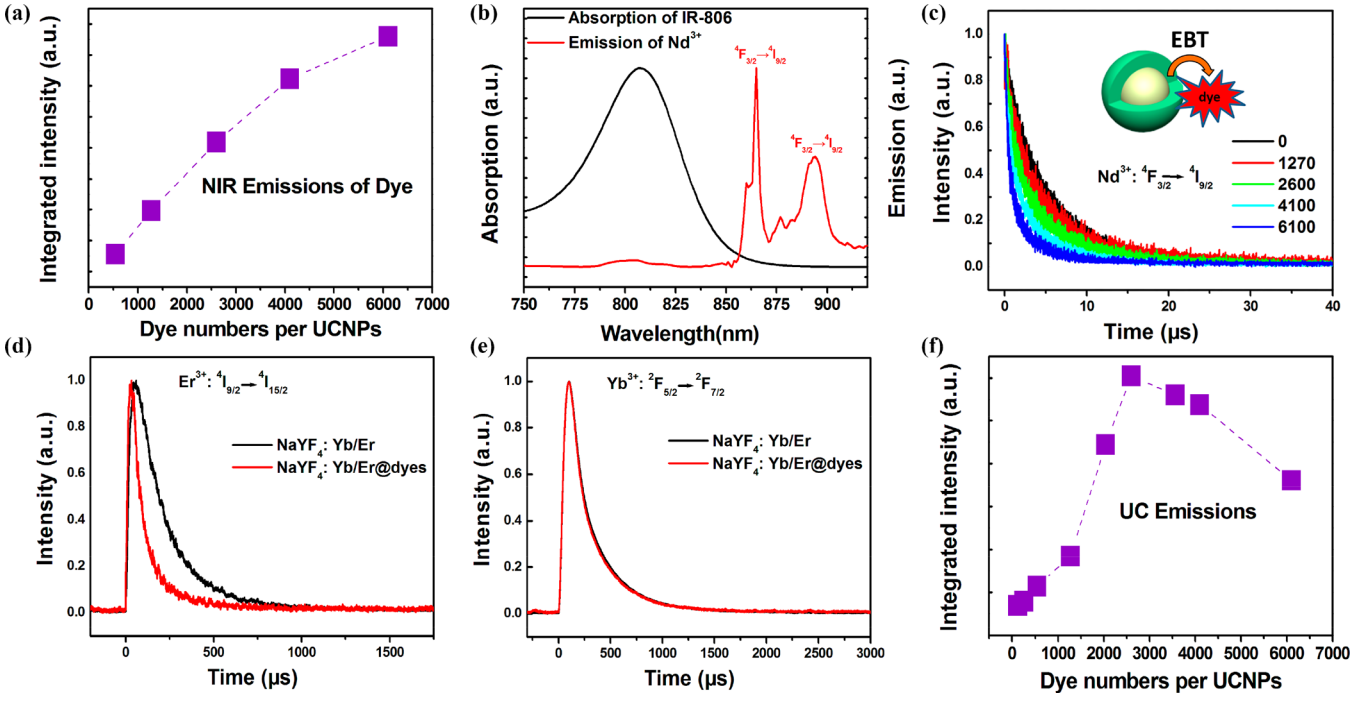

Figure 2. (a) NIR emission intensity integrated in the range of 810 to 870 nm of IR-806 sensitized UCNPs as a function of the conjugated dye numbers per UCNP. (b) Emission spectrum of Nd^{3+} and absorption spectrum of IR-806. (c) Luminescence decay curves of Nd^{3+} emission in the Nd20 CS at 863 nm with variable conjugated dyes (0−6100 per UCNP). (d) Lifetimes of Er^{3+} ($^4I_{9/2} \rightarrow {}^4I_{15/2}$, emission at ∼800 nm) of $NaYF_4$:Yb/Er nanoparticles without dyes (black lines) and with dyes (red line, ∼3000 dyes per UCNP) under 980 nm excitation. (e) Lifetimes of Yb^{3+} ($^2F_{5/2} \rightarrow {}^2F_{7/2}$, emission at ∼1040 nm) of $NaYF_4$:Yb/Er nanoparticles without dyes (black lines) and with dyes (red line, ∼3000 dyes per UCNP) under 980 nm excitation. (f) UCL intensity integrated in the range of 500−700 nm of IR-806 sensitized UCNPs as a function of the linked dye numbers per UCNP.

DOI: 10.1021/acs.jpclett.8b01931
J. Phys. Chem. Lett. 2018, 9, 4625−4631

to thousands of Ln^{3+} ions in one UCNP, but one UCNP can simultaneously interact with hundreds or thousands of strong absorptive dyes on its surface. This will lead to the absorption of one UCNP enhanced hundreds or thousands of times. However, the large enhanced absorption only resulted in several ten times enhancement of UCL,[27,29,34,35] which is confusing and must be urgently elucidated.

In this work, we chose dye-sensitized $NaYF_4$:Yb/Er@$NaYF_4$:Nd core−shell UCNPs as the basic materials to explore these issues. We carefully inspected the process of dye-sensitized UCL and obtained a clearer picture. In particular, we confirmed the existing energy back transfer (EBT) process as a new dissipate route in the dye-sensitized UCL. Moreover, we also considered the energy migration (EM) loss and theoretically simulated it in our system. On the basis of such a clear physical picture, we gave out a clear description to assess to the enhanced ability of dye sensitization, which denotes the way to obtain bright dye-sensitized UCL.

The designed system was composed of Nd^{3+}-doped epitaxial core−shell UCNPs and the surface-bonded dyes of IR-806 (Figure 1a). The dyes of IR-806 harvest large amounts of NIR light and then transfer the excitation energy to the Nd^{3+} ions due to the large spectra overlap between IR-806 and Nd^{3+} (Figure 1b).[27,32] The Nd^{3+} ions sitting in the outer shell then migrate/transfer excitation energy to Yb^{3+} in the inner core and, finally, to the activators of Er^{3+} for generating UCL. The dye-sensitized $NaYF_4$:Yb/Er (25/2%)@$NaYF_4$:Nd (20%) core−shell nanoparticles (denoted as Nd20 CS) were successfully synthesized (Figures S2−S7) based on previous reports.[19,26] Eventually, we found that after ∼2600 dyes (calculation details in the Supporting Information) were conjugated onto the surface of one UCNP, the UCL of Nd20 CS increased 44 times (Figure 1c). The similar enhancement factor was also observed in other similar works through the dye-sensitized method.[27,29,35] According to the nonlinear power dependence property of the photoluminescence (Figure 1d), the calculated population rates of UCNPs were enhanced only ∼6.6 times. However, after ∼2600 dyes were conjugated per UCNP, the absorption (at ∼808 nm) of UCNPs was enhanced ∼978 times (Figure 1e). The largely enhanced absorption and the limited enhancement factor of UCL imply that a large amount of excitation energy was not utilized by UCNPs. What happened during the process of dye-sensitization UCL?

To elucidate this enhancement gap, we first considered that the unmatched inputs and outputs may arise from the self-quenching effects of dyes themselves. If the quenching effects happened, then the absorbed excitation energies would be quenched by each other rather than transferred to UCNPs. However, the absolute NIR emission intensity of IR-806 still gradually increased with increased conjugated dyes (from 540 to 6100 dyes per UCNP, Figure 2a). The gradually increased NIR emissions and other results (Figure S8) demonstrated that heavy self-quenching effects of the dyes did not happen.

Excluding the possibility of heavy self-quenching effects, we infer that there must exist other factors that have not been considered. Surprisingly, we found that there exists EBT from the UCNPs to dyes. Actually, as shown in Figure 2b, the overlap between the emission bands of Nd^{3+} and the absorption band of IR-806 is small. This suggests that EBT from Nd^{3+} to IR-806 should also be small. Therefore, the EBT process was usually ignored. However, actually, after conjugating with thousands of dyes, the lifetimes of Nd^{3+} ($^4F_{3/2} \rightarrow {}^4I_{9/2}$) were obviously shortened (Figure 2c), which demonstrated that EBT from Nd^{3+} to dyes occurred. The sharp drop of lifetime indicated that the quenching behavior arose from dynamic ET rather than static ET (reabsorption). Furthermore, with increasing conjugated dye numbers per UCNP (1270, 2600, 4100 and 6100, respectively), the average lifetimes of Nd^{3+} were gradually shortened from 5.04 μs to 4.29, 3.42, 2.33, and 1.50 μs, respectively, evincing that the EBT process was aggravated. According to the EBT efficiency = $1 - \tau_{DA}/\tau_D$, the EBT efficiency was estimated to be 14.8, 32, 52.6, and even 70.2%, respectively.

Under the condition of little spectra overlap, this EBT still happened. According to FRET theory, the ET efficiency is defined as[36]

$$\eta = \frac{R_0^6}{R_0^6 + r^6} = \frac{1}{1 + \left(\frac{r}{R_0}\right)^6} \quad (1)$$

where r is the distance between donor and acceptor and R_0 is the Förster radius. According to eq 1, under the condition of the fixed energy-transfer distance r (fixed shell thickness ∼4 nm), we can see that η is the increase function of R_0^6. The spectra overlap determines the Förster radius R_0 according to eqs S1 and S2 of the Supporting Information. Therefore, when the spectra overlap is little, the ET efficiency will be very low, and the EBT process should not happen, and which was often ignored for most previous studies. However, for dye-sensitized UCL, the basic model is not fully corrected. From the eyes of the EBT process, dyes of IR-806 become the acceptors and UCNPs become the donors. One UCNP as the donor (∼32 nm) with large surface area can be attached to thousands of acceptors of dyes. Recognizing this point, the ET equation should be modified. Only a few studies have considered theoretical models for existing multiple acceptors in the FRET system. The most classical model is provided by Mattoussi et al.,[37] in which the ET efficiency was expressed as

$$\eta = \frac{nR_0^6}{nR_0^6 + r^6} = \frac{1}{1 + \frac{1}{n}\left(\frac{r}{R_0}\right)^6} \quad (2)$$

where n is the numbers of the acceptors. According to eq 2, apparently, the ET efficiency will be increased with the numbers of acceptors. Therefore, although the spectra overlap is small, for the EBT process, the large number of the acceptors (conjugated with thousands of dyes) as well as the strong absorption ability of dyes coresulted in the EBT process that happened.

It should be noted that although the NIR emission (∼800 nm) of Er^{3+}($^4I_{9/2} \rightarrow {}^4I_{15/2}$) was not observed in our system, the EBT from Er^{3+} to IR-806 could also occur. For example, for the $NaYF_4$:Yb/Er nanoparticles, after conjugated with ∼3000 dyes per UCNP, we found that the lifetime of Er^{3+}(∼800 nm) under 980 nm excitation was evidently shorted (Figure 2d), which demonstrated that the EBT from Er^{3+} to IR-806 in the NIR region could also exist. In addition, for Yb^{3+} ions, the emission of Yb^{3+} (∼1040 nm) is too far from the absorption of IR-806 (∼806 nm). After conjugated with ∼3000 dyes per UCNP, the lifetime of Yb^{3+} ($^2F_{5/2} \rightarrow {}^2F_{7/2}$) of $NaYF_4$:Yb/Er nanoparticles was nearly unchanged (Figure 2e), which demonstrated that EBT from Yb^{3+} to IR-806 was not efficient. Very recently, dye-sensitized DCL was fulfilled by Meijerink et al.[30] We infer that one key factor result in their success is that

DOI: 10.1021/acs.jpclett.8b01931
J. Phys. Chem. Lett. 2018, 9, 4625−4631

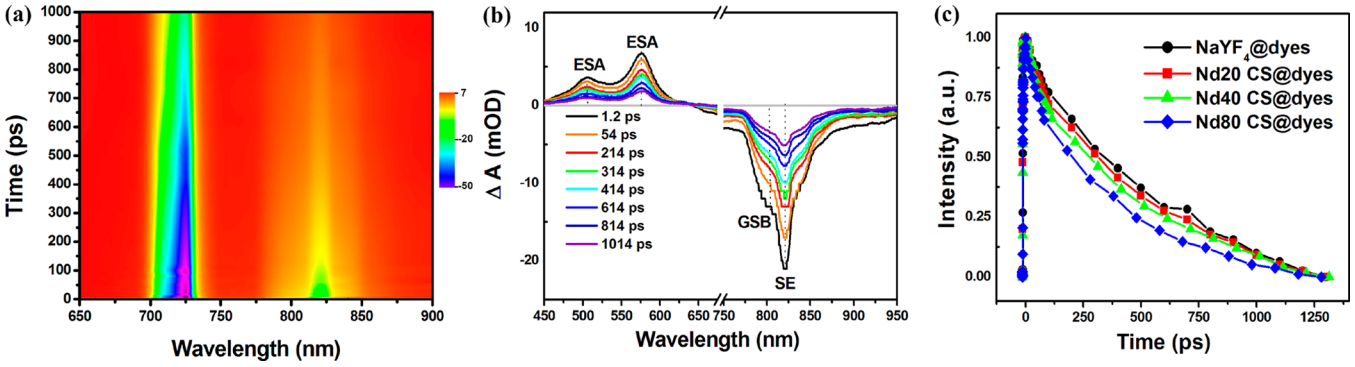

Figure 3. (a) Top view of TA data of dye-sensitized Nd20 CS UCNPs in $CHCl_3$.(b) Relative absorption variation as a function of the wavelength for time delays ranging from 1.2 to 1014 ps with 720 nm pumping for Nd20 CS UCNPs. (c) Time-resolved TA spectra of dye-linked $NaYF_4$ nanoparticles, dye-sensitized Nd20 CS, dye-sensitized Nd40 CS, and dye-sensitized Nd80 CS probed at 825 nm; all of the samples kept ~2600 dye molecules per nanoparticle.

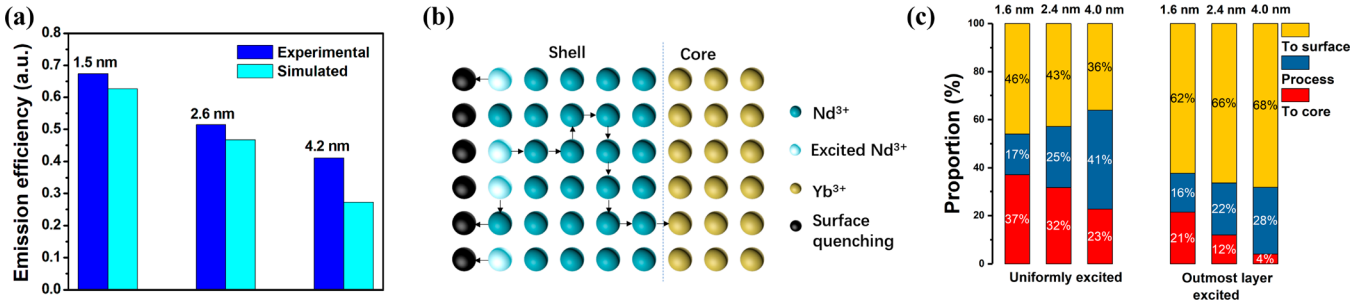

Figure 4. (a) Experimental (blue, integrated from the NIR emission of Yb^{3+} in Figure S9) and simulated (cyan) emission efficiency (means emissions are normalized to their absorption) of the UCNPs with different thickness of Nd-doped layer. (b) Schematic diagram of the simulation model in which only the outmost layer of Nd^{3+} ions was excited. (c) Proportion of excitation energy migrating to surface quenching sites (yellow), EM loss during the process of excitation energy passing through the Nd-doped layer (slate blue), and the final excitation energy migrating to the inner core (red) when the Nd-doped layer was uniformly excited (left) and only the Nd^{3+} ions in the outmost layer were excited (right).

the EBT process is very low because the downconversion emissions in their system are located in the NIR region (~980 nm), which is far away from the absorption (~400 nm) of dyes. Therefore, for dye-sensitized UCL or even DCL, the EBT process should be carefully considered, especially because the emission of Ln^{3+} closes the broadband absorption of dye.

Interestingly, when more dyes are conjugated on the surface of UCNPs, although heavy fluorescence self-quenching of dyes has not happened (Figure 2a and Figure S9) in our system, the EBT effect becomes stronger (Figure 2c), which is also unfavorable for the sensitized UCL. On one hand, conjugating more dyes will transfer more energy to UCNPs. On the other hand, conjugating more dyes will induce a heavy EBT effect to lower UCL. A trade-off of the two conflicting factors has to be reached for the optimal ratio (~2600:1) of dyes to UCNP (Figure 2f). Therefore, the EBT effect can restrict the optimal dye numbers per UCNP, which is unfavorable for dye-sensitized UCL.

We also studied the ET process from dyes to UCNPs. Transient absorption (TA) spectroscopy has been a classic method to analyze the excited-states dynamics, especially in the NIR region.[38,39] Figure 3a shows the top view of the TA spectroscopy change of dyes of dye-sensitized Nd20 CS. Figure 3b presents the according TA dynamic spectra of the dyes. According to previous reports,[40,41] the TA spectrum in Figure 3b contains three contributions: ground-state bleach (GSB), stimulated emission (SE), and excited-state absorption (ESA) (detailed explanation in the Supporting Information). Focusing on the ~825 nm signal, we obtained the effective lifetime of IR-806 (Figure 3c), which was 438, 410, 378, and 324 ps for dyes (conjugated on $NaYF_4$ nanoparticles) and dye-sensitized $NaYF_4$:Yb/Er (25/2%)@$NaYF_4$:Nd (20%) nanoparticles (Nd20 CS), Nd40 CS, and Nd80, respectively. Agreeing with eq 2, we indeed found that the ET efficiency increased with the increased doping concentration of Nd^{3+}. According to the lifetime changes of IR-806 (Figure 2c), the ET efficiency was increased from 6.4, 13.6, to 26% for dye-sensitized Nd20 CS, Nd40 CS, and Nd80 CS, respectively.

The ET efficiency was not high, which may seem reasonable in our system. According to eq 1, we can see that η is the increased function of R_0^6, and R_0^6 is determined by the quantum yield of donor and the overlap integral J. Therefore, the low ET efficiency in our system was explained by two aspects. On one hand, the quantum yield of the NIR dyes of IR-806 was tested to be only ~1.74%, which will lead to small R_0. On the other hand, as the acceptor of lanthanide ions, the ε_A of Nd^{3+} is small to extract the energy from dyes, which will result in a small overlap integral value and then small R_0. Actually, the overlap integral $J_{\text{dye-UCNPs}}$ is calculated to be 6.34×10^{11} nm^4 M^{-1} cm^{-1}, which is evidently lower than the typical overlap−integral unit (OLI = 10^{14} nm^4 M^{-1} cm^{-1}).[42] Therefore, on the basis of the discussion above, we can conclude that choosing the dyes with high quantum yield, increasing the overlap integral (enlarging the spectra overlap or choosing Ln^{3+} with strong absorption ability), and even increasing the Ln^{3+}-doped acceptors to as many as possible are the main avenues to increase the ET from dyes to UCNPs.

DOI: 10.1021/acs.jpclett.8b01931
J. Phys. Chem. Lett. 2018, 9, 4625−4631

It is well known that it is difficult for dyes to sensitize quantum dots (QDs) due to the large lifetime mismatch between QDs (often >10 ns) and dye donors (usually <10 ns).[43,44] This is because if the process of dye-sensitized QD happened, then a QD with a longer lifetime would often be in its excited state rather than ground state, and, simultaneously, dye would be in its excited state. Therefore, the number of available QD acceptors is negligible, and then the dye-sensitized QD is negligible. Whereas one feature of UCNPs that is different from QDs is that one UCNP contains many luminescence centers doped in the nanoshell. So even if one luminescence lanthanide ion is excited by dye sensitization, there still exist many lanthanide ion acceptors that remain in their ground state for further sensitization. Therefore, even for the dye donors with evidently shorter lifetimes (<1 ns) than UCNPs (>1 μs), ET can also happen due to a large number of lanthanide ion acceptors existing in one UCNP.

In addition, to fulfill UCL, the received excitation energy from dyes must experience many migration steps, which will generate EM loss. Figure 4a shows that nanoparticles with thicker Nd-doped layer generated weaker NIR emission efficiency, which demonstrated that EM loss happened when the excitation energy passed through the Nd-doped layer. Recently, we established the Monte Carlo simulation model to successfully track the EM process.[45] Similarly, we simulated the EM loss process of the Nd-doped UCNPs. The simulation results (Figure 4a, details in the Supporting Information) agree well with experimental results. Experimental and simulation results coindicated that EM loss was generated when excitation energy was across the Nd-doped layer.

More importantly, it should be noted that dyes mainly sensitize the surface ions of the nanoparticles (R_0 was calculated to be ~1 nm; details in the Supporting Information). Then, the surface ions will easily migrate excitation energy to surface quenching sites. Although this process is difficult to study experimentally, we can explore this issue through a simulation method. As shown in Figure 4b, the simulation model assumed that the outermost layer of Nd^{3+} ions of the Nd-doped layer was excited, then the EM loss was checked. For comparison, we also simulated the traditional case that the Nd-doped layer was uniformly excited. Figure 4c shows that when surface quenching effects existed, EM loss was heavier when only the Nd^{3+} ions in the outmost layer were excited. Moreover, when the surface quenching existed, most of excitation energy (beyond 60%) was migrated to the surface quenching sites. The heavy EM loss was further confirmed by performing a similar simulation with different model parameters (Figures S15−S19). In particular, if the EM rates are higher (such as highly doping Nd^{3+}), then the surface quenching effects will become heavier (Figures S15−S19). For comparison, without surface quenching sites, the simulation results showed that for the thin Nd-doped layer (such as 1.6 nm) with high migration rates, beyond 90% of the excitation energy will be utilized rather than dissipated during the EM process (Figure S20e,f). Therefore, how to decrease the heavy EM loss, especially eliminate or alleviate the excitation energy migrating to surface quenching sites, will take a massive stride in generating ultrabright dye-sensitized UCL and remains to be solved in the future.

On the basis of such a clear physical picture above, we estimated the amplified population rates of UCNPs by dye sensitization. For one dye-sensitized UCNP, the enhancement factor of the population rates P_{EF} is expressed as (details in the Supporting Information):

$$P_{EF} = (1 + A_{EF}\eta_{ET})(1 - \eta_{EBT})(1 - \eta_{EM}) \quad (3)$$

where A_{EF} is the enhancement factor of the absorption of UCNPs by dye-sensitization, η_{ET} and η_{EBT} represent the ET efficiency from dyes to UCNPs and the EBT efficiency from UCNPs to dyes, and η_{EM} represents the EM loss efficiency during the migration process. Finally, the population rates were calculated to be enhanced ~6.5-fold (details in the Supporting Information); then, the UCL should be calculated to be enhanced ~42-fold, which is similar to the experimental enhancement factor (44-fold) of UCL. Although the absorption of UCNPs was increased nearly 1000 times, the large amount of loss during the ET, EBT, and EM processes results in the final population rates being enhanced only several times. In addition, it should be noted that besides the excitation light (Figure S21a), the ~540 nm emissions can also result in photobleaching of dyes of IR-806 (Figure S21c), which may arise from the weak absorption (~500 nm) of dyes (Figure S7a). The photobleaching will also minimize the enhancement ability of dyes due to a virtual reduction of the number of dyes, which is especially unfavorable for some practical applications that need continuous irradiation.

In summary, we established the clear physical picture behind the dye-sensitized UCL process, which includes the ET, EBT, and EM processes. In particular, the ultrastrong broadband absorption of dyes and the large number of dyes conjugated on the surface of UCNPs not only resulted in ET for sensitizing UCNPs but also contributed to the high unwanted EBT from UCNPs to dyes. The high EBT process even could limit the conjugated number of dyes used for UCL. More importantly, surface-excited Nd^{3+} ions would easily migrate energy to surface quenching sites, which will generate heavy EM loss. Considering the loss during the ET, EBT, and EM processes, we reasonably explained the gap between the excitation energy input and the UCL output. Given that UCL is the nolinear power dependence property of the photoluminescence, when the absorption of UCNPs is increased 100- or 1000-fold, the UCL should be enhanced 100- to 10 000-fold theoretically. Therefore, to avoid the energy loss during the ET, EBT, and EM processes will remarkably enhance UCL, which remains a large space to explore in the future.

In addition, we have demonstrated that the acceptor number is the critical factor, which not only resulted in the ET from the dyes to UCNPs (even though the lifetime of donors is much shorter than that of acceptors) but also generated the surprising EBT from UCNPs to dyes (even though the spectra overlap is little). Actually, for dye-sensitized Ln^{3+}-doped nanoparticles, thousands of dyes can exist on the surface of nanoparticles, and the nanoparticles contain thousands of lanthanide ions as luminescence centers. Thus multiple donors and acceptors can simultaneously exist in one nanosystem, which has never been previously seen. New theoretical models and more experimental studies need to be considered in the future.

■ ASSOCIATED CONTENT

Supporting Information

The Supporting Information is available free of charge on the ACS Publications website at DOI: 10.1021/acs.jpclett.8b01931.

DOI: 10.1021/acs.jpclett.8b01931
J. Phys. Chem. Lett. 2018, 9, 4625−4631

Supporting data, materials and methods, FRET radius calculation, Monte Carlo simulation of EM process, and estimations of the enhanced population rates (PDF)

AUTHOR INFORMATION

Corresponding Authors

*J.S.: E-mail: songjun@szu.edu.cn.
*J.Q.: E-mail: jlqu@szu.edu.cn.
*Y.Z.: E-mail: zhangyl@ciomp.ac.cn.
*X.K.: E-mail: xgkong14@ciomp.ac.cn.

ORCID

Yulei Chang: 0000-0001-7223-1797
Jun Song: 0000-0002-2321-7064
Evert Jan Meijer: 0000-0002-1093-9009

Notes

The authors declare no competing financial interest.

ACKNOWLEDGMENTS

This work was financially supported by NSF of China (11374297, 61575194, 11674316, 11504371, 11604331, 61605130, 61775145, 61605124, 31771584, 61525503, 61620106016, 81727804, and 51602201), Project of Science and Technology Agency, Jilin Province (20170520113JH, 20170520112JH, and 20170519002JH), Joint research program between CAS of China and KNAW of The Netherlands, European Commission of a H2020 MSCA award under proposal number 675743 (ISPIC) and Netherlands Organization for Scientific Research in the framework of the Fund New Chemical Innovation (2015) TA under grant no. 731.015.206, and EU COST program no. 1403. Parts of this work were supported by National Basic Research Program of China (2015CB352005), Guangdong Natural Science Foundation Innovation Team (2014A030312008), and Shenzhen Basic Research Project (JCYJ20170412110212234, JCYJ20160308093035903, JCYJ20150930104948169, JCYJ20160328144746940, GJHZ20160226202139185). The work of D.S. was supported by the research program of the "Stichting voor Fundamenteel Onderzoek der Materie (FOM)", which is financially supported by the 'Nederlandse Organisatie voor Wetenschappelijk Onderzoek' (NWO).

REFERENCES

(1) Hedley, G. J.; Ruseckas, A.; Samuel, I. D. W. Light Harvesting for Organic Photovoltaics. *Chem. Rev.* **2017**, *117* (2), 796−837.
(2) Rudolf, M.; Kirner, S. V.; Guldi, D. M. A multicomponent molecular approach to artificial photosynthesis - the role of fullerenes and endohedral metallofullerenes. *Chem. Soc. Rev.* **2016**, *45* (3), 612−630.
(3) Zhu, X. J.; Su, Q. Q.; Feng, W.; Li, F. Y. Anti-Stokes shift luminescent materials for bio-applications. *Chem. Soc. Rev.* **2017**, *46* (4), 1025−1039.
(4) Qiu, X. C.; Zhu, X. J.; Xu, M.; Yuan, W.; Feng, W.; Li, F. Y. Hybrid Nanoclusters for Near-Infrared to Near-Infrared Upconverted Persistent Luminescence Bioimaging. *ACS Appl. Mater. Interfaces* **2017**, *9* (38), 32583−32590.
(5) Wang, F.; Wen, S.; He, H.; Wang, B.; Zhou, Z.; Shimoni, O.; Jin, D. Microscopic inspection and tracking of single upconversion nanoparticles in living cells. *Light: Sci. Appl.* **2018**, *7*, 18007.
(6) Li, Z. H.; Yuan, H.; Yuan, W.; Su, Q. Q.; Li, F. Y. Upconversion nanoprobes for biodetections. *Coord. Chem. Rev.* **2018**, *354*, 155−168.
(7) Liu, K.-C.; Zhang, Z.-Y.; Shan, C.-X.; Feng, Z.-Q.; Li, J.-S.; Song, C.-L.; Bao, Y.-N.; Qi, X.-H.; Dong, B. A flexible and superhydrophobic upconversion-luminescence membrane as an ultrasensitive fluorescence sensor for single droplet detection. *Light: Sci. Appl.* **2016**, *5*, e16136.
(8) Lei, X. L.; Li, R. F.; Tu, D. T.; Shang, X. Y.; Liu, Y.; You, W. W.; Sun, C. X.; Zhang, F.; Chen, X. Y. Intense near-infrared-II luminescence from NaCeF4:Er/Yb nanoprobes for in vitro bioassay and in vivo bioimaging. *Chem. Sci.* **2018**, *9* (20), 4682−4688.
(9) Dong, H.; Sun, L. D.; Feng, W.; Gu, Y. Y.; Li, F. Y.; Yan, C. H. Versatile Spectral and Lifetime Multiplexing Nanoplatform with Excitation Orthogonalized Upconversion Luminescence. *ACS Nano* **2017**, *11* (3), 3289−3297.
(10) Zuo, J.; Li, Q. Q.; Xue, B.; Li, C. X.; Chang, Y. L.; Zhang, Y. L.; Liu, X. M.; Tu, L. P.; Zhang, H.; Kong, X. G. Employing shells to eliminate concentration quenching in photonic upconversion nanostructure. *Nanoscale* **2017**, *9* (23), 7941−7946.
(11) Liu, Y. J.; Lu, Y. Q.; Yang, X. S.; Zheng, X. L.; Wen, S. H.; Wang, F.; Vidal, X.; Zhao, J. B.; Liu, D. M.; Zhou, Z. G.; et al. Amplified stimulated emission in upconversion nanoparticles for super-resolution nanoscopy. *Nature* **2017**, *543* (7644), 229−233.
(12) Zhan, Q. Q.; Liu, H. C.; Wang, B. J.; Wu, Q. S.; Pu, R.; Zhou, C.; Huang, B. R.; Peng, X. Y.; Agren, H.; He, S. L. Achieving high-efficiency emission depletion nanoscopy by employing cross relaxation in upconversion nanoparticles. *Nat. Commun.* **2017**, *8*, 1058.
(13) Chen, S.; Weitemier, A. Z.; Zeng, X.; He, L.; Wang, X.; Tao, Y.; Huang, A. J. Y.; Hashimotodani, Y.; Kano, M.; Iwasaki, H.; et al. Near-infrared deep brain stimulation via upconversion nanoparticle-mediated optogenetics. *Science* **2018**, *359* (6376), 679−683.
(14) Lin, X.; Chen, X.; Zhang, W.; Sun, T.; Fang, P.; Liao, Q.; Chen, X.; He, J.; Liu, M.; Wang, F.; et al. Core-Shell-Shell Upconversion Nanoparticles with Enhanced Emission for Wireless Optogenetic Inhibition. *Nano Lett.* **2018**, *18* (2), 948−956.
(15) Sun, L. N.; Wei, R. Y.; Feng, J.; Zhang, H. J. Tailored lanthanide-doped upconversion nanoparticles and their promising bioapplication prospects. *Coord. Chem. Rev.* **2018**, *364*, 10−32.
(16) Zuo, J.; Tu, L.; Li, Q.; Feng, Y.; Que, I.; Zhang, Y.; Liu, X.; Xue, B.; Cruz, L. J.; Chang, Y.; et al. Near Infrared Light Sensitive Ultraviolet-Blue Nanophotoswitch for Im-Guided "Off-On" Therapy. *ACS Nano* **2018**, *12* (4), 3217.
(17) Wang, P. Y.; Wang, C. L.; Lu, L. F.; Li, X. M.; Wang, W. X.; Zhao, M. Y.; Hu, L. D.; El-Toni, A. M.; Li, Q.; Zhang, F. Kinetics-mediate fabrication of multi-model bioimaging lanthanide nanoplates with controllable surface roughness for blood brain barrier transportation. *Biomaterials* **2017**, *141*, 223−232.
(18) Tan, G. R.; Wang, M. H.; Hsu, C. Y.; Chen, N. G.; Zhang, Y. Small Upconverting Fluorescent Nanoparticles for Biosensing and Bioimaging. *Adv. Opt. Mater.* **2016**, *4* (7), 984−997.
(19) Wang, D.; Xue, B.; Kong, X. G.; Tu, L. P.; Liu, X. M.; Zhang, Y. L.; Chang, Y. L.; Luo, Y. S.; Zhao, H. Y.; Zhang, H. 808 nm driven Nd^{3+}-sensitized upconversion nanostructures for photodynamic therapy and simultaneous fluorescence imaging. *Nanoscale* **2015**, *7* (1), 190−197.
(20) Li, D. H.; Liu, X. F.; Qiu, J. R. Probing Interaction Distance of Surface Quenchers in Lanthanide-Doped Upconversion Core Shell Nanoparticles. *J. Phys. Chem. C* **2018**, *122* (18), 10278−10283.
(21) Jin, L. M.; Chen, X.; Siu, C. K.; Wang, F.; Yu, S. F. Enhancing Multiphoton Upconversion from $NaYF_4$:Yb/Tm@$NaYF_4$ Core-Shell Nanoparticles via the Use of Laser Cavity. *ACS Nano* **2017**, *11* (1), 843−849.
(22) He, J. J.; Zheng, W.; Ligmajer, F. L.; Chan, C. F.; Bao, Z. Y.; Wong, K. L.; Chen, X. Y.; Hao, J. H.; Dai, J. Y.; Yu, S. F.; et al. Plasmonic enhancement and polarization dependence of nonlinear upconversion emissions from single gold nanorod@SiO_2@CaF_2:Yb^{3+},Er^{3+} hybrid core-shell-satellite nanostructures. *Light: Sci. Appl.* **2016**, *6*, e16217.
(23) Wu, D. M.; Garcia-Etxarri, A.; Salleo, A.; Dionne, J. A. Plasmon-Enhanced Upconversion. *J. Phys. Chem. Lett.* **2014**, *5* (22), 4020−4031.
(24) Chen, B.; Liu, Y.; Xiao, Y.; Chen, X.; Li, Y.; Li, M.; Qiao, X.; Fan, X.; Wang, F. Amplifying Excitation-Power Sensitivity of Photon

DOI: 10.1021/acs.jpclett.8b01931
J. Phys. Chem. Lett. 2018, 9, 4625−4631

Upconversion in a $NaYbF_4$:Ho Nanostructure for Direct Visualization of Electromagnetic Hotspots. *J. Phys. Chem. Lett.* **2016**, *7* (23), 4916−4921.
(25) Zhao, J.; Jin, D.; Schartner, E. P.; Lu, Y.; Liu, Y.; Zvyagin, A. V.; Zhang, L.; Dawes, J. M.; Xi, P.; Piper, J. A.; et al. Single-nanocrystal sensitivity achieved by enhanced upconversion luminescence. *Nat. Nanotechnol.* **2013**, *8* (10), 729−734.
(26) Zou, W. Q.; Visser, C.; Maduro, J. A.; Pshenichnikov, M. S.; Hummelen, J. C. Broadband dye-sensitized upconversion of near-infrared light. *Nat. Photonics* **2012**, *6* (8), 560−564.
(27) Chen, G. Y.; Damasco, J.; Qiu, H. L.; Shao, W.; Ohulchanskyy, T. Y.; Valiev, R. R.; Wu, X.; Han, G.; Wang, Y.; Yang, C. H.; et al. Energy-Cascaded Upconversion in an Organic Dye-Sensitized Core/Shell Fluoride Nanocrystal. *Nano Lett.* **2015**, *15* (11), 7400−7407.
(28) Wu, X.; Lee, H.; Bilsel, O.; Zhang, Y.; Li, Z.; Chen, T.; Liu, Y.; Duan, C.; Shen, J.; Punjabi, A.; et al. Tailoring dye-sensitized upconversion nanoparticle excitation bands towards excitation wavelength selective imaging. *Nanoscale* **2015**, *7* (44), 18424−18428.
(29) Wang, D.; Wang, D.; Kuzmin, A.; Pliss, A.; Shao, W.; Xia, J.; Qu, J.; Prasad, P. N. ICG-Sensitized $NaYF_4$:Er Nanostructure for Theranostics. *Adv. Opt. Mater.* **2018**, *6*, 1701142.
(30) Wang, Z. J.; Meijerink, A. Dye-Sensitized Downconversion. *J. Phys. Chem. Lett.* **2018**, *9* (7), 1522−1526.
(31) Lee, J.; Yoo, B.; Lee, H.; Cha, G. D.; Lee, H. S.; Cho, Y.; Kim, S. Y.; Seo, H.; Lee, W.; Son, D.; et al. Ultra-Wideband Multi-Dye-Sensitized Upconverting Nanoparticles for Information Security Application. *Adv. Mater.* **2017**, *29* (1), 1603169.
(32) Xu, J. T.; Yang, P. P.; Sun, M. D.; Bi, H. T.; Liu, B.; Yang, D.; Gai, S. L.; He, F.; Lin, J. Highly Emissive Dye-Sensitized Upconversion Nanostructure for Dual-Photosensitizer Photodynamic Therapy and Bioimaging. *ACS Nano* **2017**, *11* (4), 4133−4144.
(33) Wu, X.; Zhang, Y.; Takle, K.; Bilsel, O.; Li, Z.; Lee, H.; Zhang, Z.; Li, D.; Fan, W.; Duan, C.; et al. Dye-Sensitized Core/Active Shell Upconversion Nanoparticles for Optogenetics and Bioimaging Applications. *ACS Nano* **2016**, *10* (1), 1060−1066.
(34) Wei, W.; Chen, G.; Baev, A.; He, G. S.; Shao, W.; Damasco, J.; Prasad, P. N. Alleviating Luminescence Concentration Quenching in Upconversion Nanoparticles through Organic Dye Sensitization. *J. Am. Chem. Soc.* **2016**, *138* (46), 15130−15133.
(35) Shao, Q.; Li, X.; Hua, P.; Zhang, G.; Dong, Y.; Jiang, J. Enhancing the upconversion luminescence and photothermal conversion properties of similar to 800 nm excitable core/shell nanoparticles by dye molecule sensitization. *J. Colloid Interface Sci.* **2017**, *486*, 121−127.
(36) Lakowicz, J. R. *Principles of Fluorescence Spectroscopy*; Springer, 2007.
(37) Clapp, A. R.; Medintz, I. L.; Mauro, J. M.; Fisher, B. R.; Bawendi, M. G.; Mattoussi, H. Fluorescence resonance energy transfer between quantum dot donors and dye-labeled protein acceptors. *J. Am. Chem. Soc.* **2004**, *126* (1), 301−310.
(38) Bai, Y.; Olivier, J. H.; Yoo, H.; Polizzi, N. F.; Park, J.; Rawson, J.; Therien, M. J. Molecular Road Map to Tuning Ground State Absorption and Excited State Dynamics of Long-Wavelength Absorbers. *J. Am. Chem. Soc.* **2017**, *139* (46), 16946−16958.
(39) Duncan, T. V.; Susumu, K.; Sinks, L. E.; Therien, M. J. Exceptional near-infrared fluorescence quantum yields and excited-state absorptivity of highly conjugated porphyrin arrays. *J. Am. Chem. Soc.* **2006**, *128* (28), 9000−9001.
(40) Berera, R.; van Grondelle, R.; Kennis, J. T. M. Ultrafast transient absorption spectroscopy: principles and application to photosynthetic systems. *Photosynth. Res.* **2009**, *101* (2−3), 105−118.
(41) Jing, P.; Han, D.; Li, D.; Zhou, D.; Zhang, L.; Zhang, H.; Shen, D.; Qu, S. Origin of Anisotropic Photoluminescence in Heteroatom-Doped Carbon Nanodots. *Adv. Opt. Mater.* **2017**, *5* (8), 1601049.
(42) Meer, B. W. V. D.; Coker, E. G.; Chen, S. Y. S. *Resonance Energy Transfer: Theory and Data*; Wiley-VCH, 1994.
(43) Clapp, A. R.; Medintz, I. L.; Fisher, B. R.; Anderson, G. P.; Mattoussi, H. Can luminescent quantum dots be efficient energy acceptors with organic dye donors? *J. Am. Chem. Soc.* **2005**, *127* (4), 1242−1250.
(44) Diaz, S. A.; Lasarte Aragones, G. L.; Buckhout-White, S.; Qiu, X.; Oh, E.; Susumu, K.; Melinger, J. S.; Huston, A. L.; Hildebrandt, N.; Medintz, I. L. Bridging Lanthanide to Quantum Dot Energy Transfer with a Short Lifetime Organic Dye. *J. Phys. Chem. Lett.* **2017**, *8* (10), 2182−2188.
(45) Zuo, J.; Sun, D. P.; Tu, L. P.; Wu, Y. N.; Cao, Y. H.; Xue, B.; Zhang, Y. L.; Chang, Y. L.; Liu, X. M.; Kong, X. G.; et al. Precisely Tailoring Upconversion Dynamics via Energy Migration in Core-Shell Nanostructures. *Angew. Chem., Int. Ed.* **2018**, *57* (12), 3054−3058.

DOI: 10.1021/acs.jpclett.8b01931
J. Phys. Chem. Lett. 2018, 9, 4625−4631